

Compositional and Thermal Evaluation of Lignocellulosic and Poultry Litter Chars via High and Low Temperature Pyrolysis

High and Low Temperature Pyrolyzed Biochars

J. M. Novak · K. B. Cantrell · D. W. Watts

© Springer Science+Business Media, LLC (outside the USA) 2012

Abstract Inorganic elements in biomass feedstocks can influence thermochemical reactions as well as the resultant char's elemental, compositional, and thermal characteristics. Chars were produced using slow pyrolysis under low ($\leq 400^\circ\text{C}$) and high ($\geq 500^\circ\text{C}$) temperature regimes from sugarcane bagasse, peanut hulls, pecan shell, pine chips, poultry litter, and switchgrass. The chars and raw feedstocks were characterized for their elemental, structural, and thermal properties to ascertain the implications of feedstock selection and pyrolysis temperatures on these properties. Char mass yields from the six feedstocks ranged between 28% and 78% by weight while carbon yields ranged between 44% and 89%. In both instances, lower yields were obtained with increasing pyrolysis temperature. Higher pyrolysis temperatures ($\geq 500^\circ\text{C}$) resulted in more neutral to alkaline chars possessing greater ash contents and increased aromatic character with narrow O/C and H/C ratios. A significant exponential curve response ($r^2=0.87$, $P<0.001$) was revealed between char mass yields vs. pyrolysis temperature. All raw feedstocks and chars contained mixed amounts of macro-, micro-, and trace element concentrations. The higher heating values (HHV) tended to increase with heightened pyrolysis temperature with some chars producing $>30 \text{ MJ kg}^{-1}$. The chars' HHV values inversely correlated to their total ash and Cl content. Lignocelluloses chars had better thermal characteristics and lower ash quality concerns implying suitable service in thermal

energy production. In contrast, poultry litter char had greater ash contents, medium HHV values, and contained corrosive inorganic elements, which rendered it problematic as a feedstock for thermal energy generation.

Keywords Bioenergy · Energy content · GRACEnet · Nuclear magnetic resonance · Thermogravimetric analysis

Abbreviations

BG	Bagasse
DTA	Differential thermal analysis
FC	Fixed carbon
HHV	Higher heating value
NMR	Nuclear magnetic resonance
PC	Pine chip
PH	Peanut hull
PL	Poultry litter
PS	Pecan shell
SW	Switchgrass
TGA	Thermal gravimetric analyzer
TG	Thermogravimetry
VM	Volatile matter

Introduction

Both lignocellulosic and poultry litter feedstocks have undergone extensive bioenergy production evaluations using thermochemical conversion platforms such as co-firing, gasification, and both slow and fast pyrolysis to produce fuel products in gas, liquid, and solid fuel phases [1–5]. Among these thermochemical conversion platforms, pyrolysis is regarded as an effective method of processing biomass to produce a combination of char, non-condensable

J. M. Novak (✉) · K. B. Cantrell · D. W. Watts
United States Department of Agriculture,
Agricultural Research Service,
Coastal Plains Research Laboratory,
2611 West Lucas St.,
Florence, SC 29501, USA
e-mail: jeff.novak@ars.usda.gov

gases, and hydrocarbon-rich bio-oil [6]. Slow pyrolysis involves carbonizing the feedstock under a very low oxygen atmosphere using temperatures between 300 and 700°C, and heating ramps of 1 to 20°C min⁻¹ lasting for a few hours to a few days [7]. In contrast, fast pyrolysis employs rapid exposure (1 to 5 s) of the feedstock to heat at temperatures between 350 and 600°C [8]. Portions of the volatiles emitted during both processes are later re-condensed downstream into bio-oil, while the solid residue is called char.

Chars produced from thermochemical processes can find utility as a substitute fuel for heat production [2, 9] or as a soil amendment [10–12]. Chars made from lignocellulosic and animal litter feedstocks will contain organic-C substances, but will also contain inorganic elements such as N, P, Cl, Na, Si, S, and K. Their concentrations in chars will vary due to differences in crop nutrient uptake [13], fortification levels in animal feed [14], and by chemicals added to livestock bedding material [15]. In addition, differences in char's elemental composition are linked to pyrolysis temperature variations employed during thermal conversion [15–18].

The presence of certain inorganic elements is deemed an obstacle for char's use as an efficient fuel source [3, 4]. Reports in the literature reveal that K, Na, Cl, and SO₄ in chars cause corrosion, fouling, deposition, slagging, sintering, and agglomeration reactions in downstream processing equipment during pyrolysis [19] as well as influencing yields of both volatile compounds [20, 21] and char [22, 23]. To minimize opportunities for these reactions to occur, it is important to utilize the appropriate feedstock and temperature during pyrolysis. In turn, the thermal production system can run more efficiently since the technical difficulties associated with certain elements can be adroitly avoided.

Feedstock selection and thermal processing conditions could be important decisions for the nascent biofuel industry in the Southeastern USA where biomass sources are abundant. The Southeastern USA has one of the highest national rates of net primary biomass productivity [24]; in turn, it is viewed as capable of supplying the majority (50%) of grasses, herbaceous crops, and forest feedstocks for the entire USA biofuel production [25]. Moreover, the animal production industry in four southeastern states (i.e., AL, GA, NC, and SC) is quite large; thus, collective manure production in these states is large with over 73 million Mg as excreted per year [26]. However, there is limited information on the impact of pyrolysis temperatures on char's compositional quality and thermal energy characteristics made from feedstocks common to the Southeastern USA. We hypothesize that the chemical composition of lignocellulosic and poultry litter feedstock will influence the pyrolytic efficiency of bioenergy generation and the char's chemical characteristics. The objectives of this research are

to produce chars by pyrolyzing lignocellulosic and poultry litter feedstocks under high and low temperature regimes and to examine their impact on char yield and their elemental, structural, and thermal characteristics.

Materials and Methods

Feedstock Selection

All of the feedstocks processed as part of this study are representative for the available feedstocks in the Southeastern United States and were collected and processed in a manner that is consistent with what would be envisioned for a large-scale pyrolysis operation. Several USDA–ARS and university teams were involved in a multi-location study to process feedstocks grown or obtained from operations in the Southeastern USA into chars to examine their quality [12]. In turn, the chars used in this study were produced at five facilities: peanut hull (PH) char at the University of Georgia; poultry litter (PL) char at the USDA–ARS Southern Regional Research Center, New Orleans, Louisiana; pecan shell (PS) and switchgrass (SW) chars at North Carolina Agricultural and Technical State University; and sugarcane bagasse (BG) and pine chip (PC) char at the USDA–ARS Coastal Plain Research Center, Florence, South Carolina (Table 1).

Pyrolysis of Feedstocks

All feedstocks required considerable processing before pyrolysis including air-drying, grinding, and sieving to pass a 6-mm sieve. These feedstocks were pyrolyzed either in a low ($\leq 400^\circ\text{C}$) or a high ($\geq 500^\circ\text{C}$) temperature regime to yield different structural and surface characteristics using procedures previously described [12, 17, 27–29].

To carbonize the feedstocks using the box furnace-retort system (Table 1), between 0.5 and 1.5 kg of ground material was loaded onto a stainless steel tray or into a crucible and placed into a gas tight retort (Lindberg/MPH, Riverside, MI) for 1 to 2 h under a stream of N₂ gas at the desired pyrolytic temperature. Char made from SW at the lower pyrolysis temperature regime (in this case 250°C) was carbonized using an 8-h residence time to ensure devolatilization of compounds and parent carbon conversion into char. This lower temperature provided a torrefied-like product expected to contain semi-degraded cellulose and hemi-cellulose compounds, since 300 to 400°C was the critical temperature for their structural breakdown [6]. Torrefaction is a similar pyrolytic process performed on feedstocks, except it is conducted under a milder (200 to 300°C) temperature regime [30]. This process was established in the forestry industry for densification of woody biomass to reduce transportation

Table 1 Description of feedstocks and pyrolysis conditions

Feedstock	Collection location	Pyrolysis (°C)	Furnace	Residence time (h) ^a	Method reference
Bagasse (hybrid <i>Saccharum</i> spp.)	Canal Pt., FL	0	Lindberg electric box with retort	0	[27]
		350		2	
		500		2	
Peanut hull (<i>Arachis hypogaea</i>)	Tifton, GA	0	Heated rotary drum	0	[18]
		400		1 to 2	
		500		1 to 2	
Pecan shell (<i>Carya illinoensis</i>)	Lumberton, NC	0	Lindberg electric box with retort	0	[15]
		350		1 to 2	
		700		1 to 2	
Pine chip (<i>Pinus taeda</i>)	Cordesville, SC	0	Lindberg electric box with retort	0	[27]
		350		2	
		500		2	
Poultry litter (<i>Gallus domesticus</i>)	Starkville, MS	0	Lindberg electric bench with retort	0	[28]
		350		1 to 2	
		700		1 to 2	
Switchgrass (<i>Panicum virgatum</i>)	Darlington, SC	0	Lindberg electric box with retort	0	[29]
		250		8	
		500		1 to 2	

^a Residence time that feedstock was pyrolyzed in furnace at maximum desired pyrolysis temperature

costs [31]. The torrefied product was a material with a larger heating value than the original feedstock that was suitable for coal-blending and subsequent co-combustion [32–34]. In spite of the classification differences, we chose this lower temperature threshold to have a different char-like material. Its inclusion in our study, therefore, allowed for comparison of materials obtained under a wide range of pyrolytic conditions. As indicated in Table 1, char from PH was produced using a heated rotary drum also employing a 1- to 2-h residence time [17]. The rotary drum was filled with several hundred kilograms of dry PH that was then carbonized into char. After removal, the char mass yield (wt.% dry basis, db) was calculated as a percentage ratio of the mass of raw feedstock input (db) and char mass output (char mass db/feedstock mass db). Afterwards, all chars were ground to pass a 0.25-mm sieve and stored in a dessicator to minimize adsorbed water surface effects.

Feedstock and Char Characterization

All raw feedstocks and char samples were characterized for pH, HHV, ultimate, proximate, and total elemental composition. The pH was determined using a 1:2 ratio of char to di. H₂O (wt v⁻¹) as described [12]. Proximate, ultimate, and HHV analyses were performed by Hazen Research Inc. (Golden, CO, USA) following ASTM D 3172, 3176, and 5865, respectively [35]. Proximate analyses provided a sample's moisture, ash, volatile matter (VM), and fixed carbon (FC) content. Meanwhile, the ultimate analysis for a biomass sample determined the C, N, H, S, and O (by

difference) content. The char C recovery on a dry, ash-free basis (daf) was calculated by a percentage ratio of C mass output and char C mass input. The chars C, H, and O contents were used to determine molar ratios, thus providing a gross structural change evaluation between raw feedstock and chars across pyrolysis temperature regimes.

The elemental composition of the raw feedstock and chars were categorized as macro (g kg⁻¹), micro (mg kg⁻¹) based on their concentration differences, and trace elements listed under Title 40, Part 503, Code of Federal Regulations [36] to determine pollutant concentration. While only one replicate was ran on the raw feedstock, triplicate samples of each char on an oven dry basis were digested using EPA 3052 microwave-assisted acid digestion method [37]. The digestions were analyzed using an inductively coupled plasma spectrometer as outlined [12] with the constituents sorted into macro: Al, Ca, Fe, K, Mg, Na, Si, and P; micro: B, Cl, Co, Cu, Mn, Se, Sn, V, and Zn; and a trace element category: Ag, As, Cd, Cr, Ni, and Pb. Total Si in a single sample of each char was determined using ASTM D 2795-86 [35] by initially fusing it with NaHO₂ in a Zr crucible, followed by dissolution in dilute HCl. The prepared liquid sample was then analyzed for total Si using a Perkin-Elmer AAnalyst 300 atomic absorption spectrophotometer (Perkin Elmer, Waltham, MA, USA). Total Cl concentrations in each char were determined using ASTM D 2361 [35]. The sample was combusted in an oxygen bomb containing 1 M NaOH. After cooling, the resultant solution containing NaCl was acidified with HNO₃ and then titrated with AgNO₃ using a Mettler DL 21 autotitrator (Mettler-Toledo, Columbus, OH, USA).

For each char, a finer-scale assessment of functional group diversity and core-structural characteristics were gathered using ^{13}C nuclear magnetic resonance spectroscopy (NMR) using a Bruker DSX-300 NMR spectrometer (Karlsruhe, Germany) operated at a ^{13}C frequency of 75.5 Mhz. Operating conditions, spectral fine tuning, and spectral interpretation were described [38]. The spectral area for each char was thus divided into aliphatic-C (0–163 ppm), aromatic-C (163–190 ppm), and carboxylic-C (190–220 ppm). The ^{13}C NMR spectra of the PL char at 700°C had a poor signal-to-noise ratio due to resonance interferences caused by ferro-magnetic species; thus, no spectrum was recorded.

The oxidative degradation (combustion) properties for each raw feedstock and char samples were analyzed in duplicate using a thermogravimetric (TG) analyzer (TGA/DSC1; Mettler Toledo International, Inc., Columbus, OH, USA) operating under a three-point calibration using In, Al, and Au as standards. All samples were placed in a 70- μL aluminum oxide crucible and dried as described [39] to allow for results assessed on a dry-weight basis. These samples were then heated under a constant 10°C min^{-1} temperature ramp from 40 to 950°C. Here, the mass loss and temperature changes (differential thermal analysis, DTA) of the samples were simultaneously recorded while being oxidized under 60 mL min^{-1} flow of zero-grade air. All DTA curves accounted for instrumental effects using version 9.10 of STARe software (Mettler Toledo International, Inc., Columbus, OH). Enthalpy changes during combustion (ΔH) were calculated by integration of the area below the DTA curve between desired temperatures using the STARe software.

Characteristic zones and temperatures defined on the TG, DTA, and DTG (rate of mass loss; derivative of TG) curves were based on [40–42]: $T_{2.5\%}$ and $T_{97.5\%}$ temperature associated with 2.5% and 97.5% of the total weight loss, respectively; T_i and DTG_i , temperature and rate of mass loss associated with maximum rate of mass loss during active (volatile) combustion zone ($i=\text{V}$) and char combustion zone ($i=\text{C}$). The onset temperature of combustion, T_{onset} , was defined as the temperature associated with the intersection of lines tangent to the (1) baseline and (2) initial slope of the first DTA curve passing through the first maxima. The temperature and change in temperature for the maximum DTA peak during volatile (subscript $i=\text{V}$) and char (subscript $i=\text{C}$) combustion zones on the DTA curve was represented as $T_{i\text{Max}}$ and $\Delta T_{i\text{Max}}$, respectively. The final characteristic temperature was T_{Endset} representing the temperature associated with the intersection of lines tangent to the ending baseline and slope of the final DTA curve passing through the maxima.

Combustion reaction kinetic parameters were determined from the TGA data based on the following rate expression

(Eq. 1) where the rate constant (k) changed with absolute temperature (T) according to the Arrhenius equation (Eq. 2):

$$\left(\frac{dX}{dt}\right) = -k X^n \quad (1)$$

$$k = A \exp\left(\frac{-E_a}{RT}\right) \quad (2)$$

here X is the weight of sample undergoing the reaction; n is the order of the reaction; A is the pre-exponential factor; E_a is the energy of activation; R is the universal gas constant (8.314 J mol^{-1} K^{-1}). Presented in a linearized form [43], Eqs. 1 and 2 become

$$\ln\left(-\left(\frac{-1}{X_o - X_f}\right)\left(\frac{dX}{dt}\right)\right) = \ln(A) - \left(\frac{E_a}{RT}\right) + n \cdot \ln\left(\left(\frac{X - X_f}{X_o - X_f}\right)\right) \quad (3)$$

Where X_o is the initial weight of the sample and X_f is the weight of the residue. The values of A , E_a , and n were determined from the TGA curves using least sum of squares.

Statistics

The impact of pyrolysis temperature on char recovery was examined by collectively ($n=12$) plotting pyrolysis temperature vs. char yields on both a mass (wt.%_{db}) and a C basis (wt.%_{daf}). The plots were then evaluated using both simple linear and polynomial regression (exponential decay) models to ascertain the best predictive fit between these variables. The best fit model was selected based on the highest r^2 value and the most significant P value obtained.

Two approaches were used to examine the influence of the char's elemental composition on yields. In the first, the total ash concentration expressed as a wt.%_{db} in each of the 12 chars were compared to the char yields expressed on a mass and C basis using a Pearson Product Moment correlation analysis. Secondly, the test procedure was repeated except the wt.%_{db} of individual inorganic elements (e.g., Ca, Si, Cl, etc.) in the 12 chars were correlated against yields expressed on both a mass and C basis.

To test if pyrolysis temperature regime had a significant effect on macro-, micro- and trace element concentrations in each char, their mean concentrations ($n=3$) were compared by temperature (high vs. low °C) per feedstock using a one-way ANOVA at a $P=0.05$ level of significance.

A Pearson Product Moment correlation test was initially used to determine if the chars' HHV measurements were dependent on their total ash content and the concentration of individual elements. Next, significant variables, as identified in the Pearson Product Moment correlation test, were further used in both linear and polynomial regression

models to refine char thermal relationships with their ash contents and the individual elemental contents.

Energy contents of the raw feedstocks and chars were tested for significant differences and if their HHV and ΔH were temperature regime dependent using a one-way ANOVA. Correlations were also used to examine relationships between proximate concentrations in each char and raw feedstock with results obtained from TG and DTA analyses. All statistical tests were performed using either SigmaStat v. 3.5 software (SSPS Corp., Chicago, IL, USA) or version 9.2 of Statistical Analysis Systems (SAS Institute Inc., Cary, NC, USA).

Results and Discussion

Char Yields

Char yields expressed on a mass and C basis were higher for all feedstocks using the lower pyrolysis temperature regime (Fig. 1a, b). Pooling char mass yields across these feedstocks ($n=6$) showed that the mean yield was 51.3% (SD=14.9) using the lower pyrolysis temperature compared to a mean yield of 31.7% (SD=3.3) at the higher temperature. Similarly, char yields on a C basis were higher (mean 67.6%, SD=11.7) using the lower pyrolysis temperature regime compared to the higher temperature (mean 51.6%, SD=4.1). This was not unexpected because pyrolysis at higher temperature using lignocellulosic materials [6, 44, 45] or animal manure [46, 47] as feedstocks undergo a series of physically and chemically destructive reactions during carbonization. Our char mass yield percentages, after comparing to other studies employing similar feedstocks and operating conditions, were comparable to char mass yields from PL, PH, and PC feedstocks [17], for nut shell feedstock [45], and from grasses and BG [2, 48].

In this study, the highest char mass yield was almost 80% from SW at 250°C, whereas the lowest yield was obtained from BG pyrolyzed at 500°C (Fig. 1a). Pyrolysis of the other four feedstocks, in comparison, had char mass yields that ranged between 30%_{db} and almost 60%_{db} (Fig. 1a). Char % yields expressed on a C basis (Fig. 1b) were slightly higher, but the same temperature trends occurred. When expressed on a mass or a C yield basis, the most char was recovered by carbonizing SW at 250°C. This lower temperature regime resulted in less dehydration and losses of VM relative to SW char made at the higher temperature (Table 2).

To establish predictable trends of char yields with pyrolysis temperature, both linear and polynomial regression analyses were used to obtain the best predictive model fit. There was a significant ($P=0.002-0.009$), but poor regression

fit ($r^2=0.51-0.63$) when ascribing a general linear model to plots of char yield expressed on a %_{db} mass or C basis vs. pyrolysis temperature (plot not shown). Further analyses using a polynomial model (exponential decay), in contrast, revealed a significant curve linear response between variables that predicted both char yields reasonably well (Fig. 1a–b, $r^2=0.87-0.89$ and $P<0.001$). For the six feedstocks used in this study, this implied that both char yields had a curve linear dependence on pyrolysis temperature. Yan et al. [49] also reported an exponential relationship between char yield obtained from southern pine and pyrolysis temperature. This significant relationship allows for selection of an appropriate pyrolysis temperature to obtain a predictable yield. Using this relationship, for example, shows that if higher char mass yields are sought, then the choice feedstock should be pyrolyzed using the lower temperature regime (250 to 400°C). This finding was similar to Demirbas [16] who reported that pyrolysis temperature during carbonization of agricultural residues significantly influenced their yields.

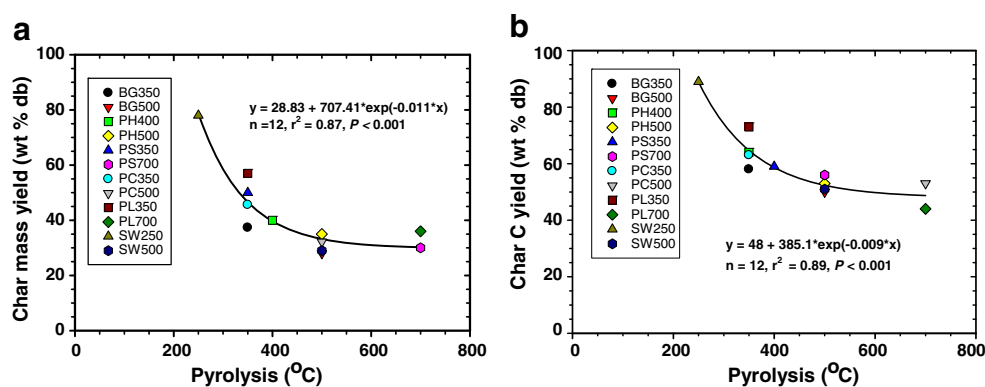
Raw Feedstock and Char Compositional Characteristics

Chemical Properties

For the six feedstocks, increasing the pyrolysis temperature to $\geq 500^\circ\text{C}$ resulted in chars having alkaline pHs and greater ash contents (Table 2). In fact, the pH values in most of the chars obtained using the higher temperature regime were between 9 and 10. The exceptions were for BG and PC 500°C chars with a pH of 6.7 (Table 2). The ash contents were lowest in chars made from pine chips ($<25\text{ g kg}^{-1}$), with chars produced from BG, PH, PS, and SW showing relatively moderate levels ($<100\text{ g kg}^{-1}$), while the greatest ash content occurred in the 700°C PL char ($<525\text{ g kg}^{-1}$). The VM and FC contents of the chars behaved inversely with respect to one another with increasing pyrolysis temperature: increases in pyrolytic temperature caused decreases in VM and increases in FC. Volatile matter is easily removed in pyrolysis and combustion processes. However, the energy density of VM may not be as great as that of FC. As demonstrated by Bridgeman et al. [42], increases in FC directly correlated to increases in overall ΔH (from DTA analysis). In this study, correlations for calculating HHV from the proximate analysis of biomass, including chars, lend FC values to be twice the weight of HHV as compared to VM [50]. Thus, the greater the FC content, one would expect a more energy dense fuel source.

The composition of the raw feedstocks contained a range of C, H, O, N, and S concentrations and was provided for baseline comparisons with corresponding elements in each char (Table 2). Inspecting the magnitude of these elements in the raw feedstocks showed, in general, that they were lower than their char equivalents. After raw feedstock

Fig. 1 Curve linear relationship between pyrolysis temperature and char yields on a mass (a) and a C (b) basis where sugarcane bagasse (BG), peanut hull (PH), pecan shell (PS), pine chips (PC), poultry litter (PL), and switchgrass (SW) feedstocks (pyrolysis temperature in degrees Celsius expressed after feedstock abbreviation)



pyrolysis, however, some elements in char will be concentrated due to loss of VM, while some elements will experience concentration declines. This was apparent when inspecting the chars' C contents, which in general were concentrated, while the H and O contents both decreased with increasing temperature. The C content during carbonizing raw PS feedstock into char, for example, increased from 516 to 912 g kg⁻¹ by raising the pyrolysis temperature. The one exception, however, was the C content in the raw PL feedstock and both chars that changed slightly (362 vs. 440 g kg⁻¹). Compared to the raw feedstocks, all chars experienced declines in their H and O concentration because of carbonization and dehydration reactions during pyrolysis.

The N contents in the chars varied greatly (Table 2). Among the feedstocks, chars made from PC and PS both had the lowest N contents (<5 g kg⁻¹). Meanwhile, PL char contained the greatest N and S amounts among the chars, probably as a result of the litter containing uric acid and undigested proteins [51] and being treated with a sodium-bisulfate (NaHSO₄) amendment to minimize NH₃ volatilization [15]. The high S contents in the PL feedstock and char is a concern because S can accentuate thermal fouling issues in downstream equipment. It would be prudent to discern if poultry litter is treated with S-containing amendments before its consideration as a feedstock for pyrolysis.

Table 2 Chemical properties of raw feedstocks and biochars ($n=1$, dry basis, VM volatile material, FC fixed C)^a

Feedstock	Pyrolysis (°C)	pH	Ash g kg ⁻¹	VM	FC	C	H	O ^b	N	S
Bagasse	0	5.3	54	847	99	481	55	406	3.6	0.4
	350	5.5	38	406	556	752	46	158	6.6	0.6
	500	6.7	44	346	610	854	33	61	7.9	0.6
Peanut hull	0	5.4	33	781	186	507	61	381	17	0.9
	400	7.9	82	384	534	748	45	97	27	0.9
	500	9.9	93	181	726	818	29	33	27	1.0
Pecan shell	0	4.8	16	785	199	516	57	410	3.0	0.2
	350	4.6	24	616	360	645	53	28	3.0	0.1
	700	9.1	52	97	851	912	15	16	2.6	0.1
Pine chip	0	3.9	8	835	157	530	59	401	2.3	<0.1
	350	4.4	15	464	521	747	50	184	4.5	0.1
	500	6.7	23	473	504	872	36	65	4.3	0.1
Poultry litter	0	8.4	244	678	78	362	48	244	41	3.2
	350	7.7	359	363	278	461	37	86	50	7.8
	700	9.6	524	141	335	440	2.5	0.1	28	8.8
Switchgrass	0	5.8	22	848	130	483	62	427	5.1	0.5
	250	6.4	26	767	207	553	60	356	4.3	0.5
	500	9.2	78	134	788	844	24	43	10.7	0.6

^a Portions of these results were previously published in [15]

^b Calculated according to ASTM D 3176 as 100 minus the sum (C-H-N-S-ash)

Char Molar Ratios and Structural Composition

It is beneficial to characterize the structural make-up of chars because the content of aromatic and O-containing polysaccharides can influence (1) its reactivity during thermal processing [49, 52] and (2) its ability to act as an effective soil C sequestration agent by resisting microbial oxidation [46, 53]. Moreover, assessment of the quality/quantity of structural and O-, H-containing functional groups in chars prepared under specific conditions allows for the refinement of biomass conversion technologies to obtain more thermally reactive chars. Therefore, each char's gross and fine-scale structural changes were investigated as a function of pyrolytic temperature regimes. As shown in Fig. 2, the widest O/C and H/C molar ratio differences occurred in the SW char processed at 250°C, which was consistent with the minimal loss of O and H (Table 2). For all other chars, however, a striking narrowing in these ratios occurred with increasing pyrolysis temperature. Chars processed under increasing pyrolysis temperature from 250 to 700°C resulted in an O/C and H/C molar ratio decline, respectively from 0.3 and 1.0 (PS at 350°C) to between 0.01 and 0.1 (PL at 700°C). The diminishing O/C and H/C ratios for all chars were consistent with previous chemical results showing loss of H and O (Table 2) and lower char yields (Fig. 1) with increasing pyrolysis temperature.

The %C distribution among the three structural groups for the 12 chars were plotted in a ternary diagram (Fig. 3). The diagram shows conspicuous modifications in structural characteristics as a function of pyrolytic temperature regime. For example, pyrolysis in the lower temperature regime ($\leq 400^\circ\text{C}$) was shown to result in chars retaining a larger portion of their VM compounds, which are mostly aliphatic-C structures (35% to 63% C distribution). Chars pyrolyzed at this lower temperature regime have a distinctly different

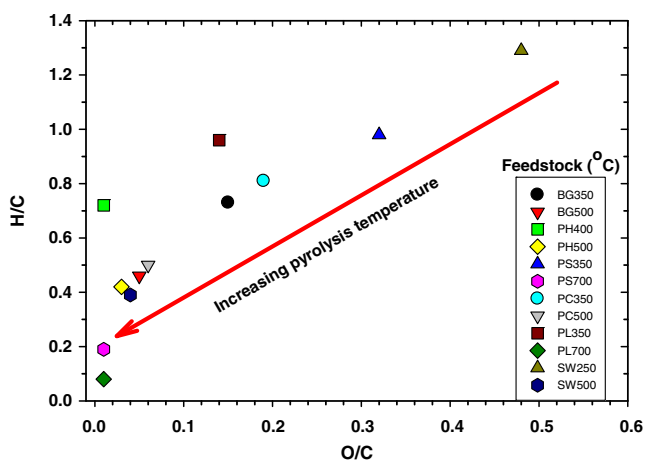


Fig. 2 Van Krevelen diagram showing molar O/C and H/C ratios for each char as a function of pyrolysis temperature (arrow indicates direction of increasing temperature)

structural make-up than chars produced at the higher temperature regime ($\geq 500^\circ\text{C}$). Pyrolysis at the higher temperature regime ($\geq 500^\circ\text{C}$) resulted in more devolatilization of organic compounds (i.e., aliphatic, O-containing polysaccharide-type, etc.) from the char's matrix. For example, the C distribution in aromatic-C structures for chars produced between 250 and 400°C ranged from 29% to 57%, which increased to between 50% and 82% at pyrolytic temperatures greater than 500°C. Per agreement with the H/C and O/C molar ratio results (Fig. 2), higher temperature pyrolysis ($\geq 500^\circ\text{C}$) favors chars composed mostly of poly-condensed aromatic structures [54–57].

Structural analyses reveals that chars lose their thermal reactivity by loss of O-containing functional groups and by a predominance of aromatic structures; therefore, choice of pyrolysis temperature for processing raw feedstocks depends on the end use of the char.

Inorganic Composition

Quantifying the macro-elemental composition of raw feedstocks and the subsequent chars has significance for the thermal energy and agricultural sectors. Some macro-elements (i.e., Ca and K) present in the raw feedstock matrix can influence the thermal reactivity of chars by acting as a catalyst [4], while other macro-elements (i.e., Na, Cl, S, and Si) can interfere with downstream thermal energy processing [19, 59, 60]. As a soil amendment, however, chars with a preponderance of Ca, K, Mg, K, P, etc. concentrations can supply soil with nutrients for crop fertilization [53].

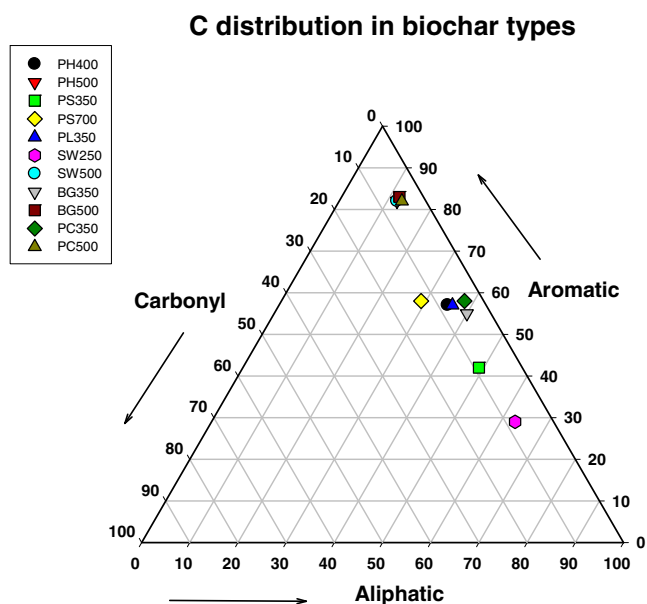


Fig. 3 Ternary diagram exhibiting C distribution among aliphatic, aromatic, and carbonyl groups in each char (the NMR spectra for PL 700°C biochar was unobtainable)

In this study, each raw feedstock (Tables 3, 4, and 5) had relatively high Ca, K, Mg, and P concentrations, with raw PL containing some of the highest Na and P concentrations (Table 3). Among the micro-elements, raw PL also had the relatively greatest amounts of Cu, Mn, and Zn, whereas raw PS contained the next greatest amounts of Cu and Zn (Table 4). The remaining raw feedstocks had mixed amounts of macro- and micro-elements, but raw PC contained some of the lowest concentrations (Tables 3 and 4).

After pyrolysis of the six raw feedstocks, the macro- and micro-elemental concentrations in the chars varied considerably. For example, Ca and K concentrations in chars from the five plant- and wood-based feedstocks (all, except PL) were the greatest among the macro-elements (Table 3). There were relatively medium P and Mg concentrations in the chars among the same five feedstocks with lower amounts of Al, Fe, and Na (Table 3). Amid the micro-nutrients, all chars contained mixed levels of Ba, Co, Cu, Mn, Mo, and Zn, but the presence of B, Se, Sn, and V were sporadic (Table 4). Among the 12 chars, Cl, Cu, Mn, and Zn concentrations were greatest in chars produced from PL feedstock (Table 4). The assortment of macro- and micro-elements in the PL chars suggests that it is a suitable soil amendment for fertility improvements; however, it has

several undesirable elements that can interfere with thermal energy production. The presence of K, Si, S, and Cl in the PL chars can reduce thermal conversion efficiencies and increasing corrosion issues [3]. On the other hand, PC and PS char have lower macro-element concentrations and could serve as a more optimum feedstock for thermal energy production.

The assortment of macro- and micro-elements along with their relatively high concentrations in this raw PL feedstock was not surprising. As noted with S levels in Table 2, poultry feed can be over-fortifying with both macro- and micro-element to account for losses via unassimilated elements excreted by poultry [14]. This action probably caused the PL chars in this study to contain various elements.

Pyrolyzing the six feedstocks into chars at the higher temperatures produced mixed results with respect to concentrating macro-elements (Table 3). On one hand, pyrolysis at higher temperature levels caused Ca in PC and Fe in PH concentration reductions, probably due to thermal instability of the associate atoms or by loss via ion-pair formation via devolatilization [3, 51, 58]. Conversely, pyrolysis of PL feedstock at the higher temperature resulted in that char's containing significantly higher K, Na, and P concentrations.

In this study, the concentrations of micro-elements in the chars varied widely between feedstock and pyrolysis

Table 3 Macro-elemental composition in raw feedstocks and chars produced under different pyrolysis temperatures (standard deviation in parentheses)

Feedstock	Pyrolysis (°C)	Macro-elements (g kg ⁻¹) ^b								
		Al	Ca	Fe	K	Mg	Na	P	Si ^a	
Bagasse	0 ^a	0.29	0.90	0.23	1.44	0.35	0.01	0.28	19.5	
	350	0.11 (0.01)a	2.04 (0.15)a	0.26 (0.004)a	3.78 (0.05)a	0.84 (0.02)a	0.03 (0.02)a	0.50 (0.06)a	11.6	
	500	0.18 (0.03)b	3.28 (0.69)b	0.34 (0.009)b	5.01 (0.10)b	0.89 (0.02)b	0.03 (<0.01)a	0.63 (0.07)a	15.9	
Peanut hull	0 ^a	0.48	1.64	0.23	5.94	0.82	<0.01	0.69	4.2	
	400	2.69 (0.41)a	5.21 (0.26)a	1.79 (0.04)a	18.55 (0.14)a	2.63 (0.47)a	0.06 (<0.01)a	2.58 (0.03)a	8.3	
	500	2.99 (0.50)a	6.22 (0.30)b	1.22 (0.33)b	19.09 (0.60)a	2.97 (0.32)a	0.09 (<0.01)b	2.61 (0.02)a	12.5	
Pecan shell	0 ^a	0.03	6.21	0.23	2.11	0.29	0.07	0.13	0.2	
	350	0.04 (0.01)a	11.0 (0.01)a	0.01 (0.01)a	2.34 (0.17)a	0.32 (0.01)a	0.10 (0.005)a	0.25 (0.15)a	0.2	
	700	0.03 (<0.01)b	23.3 (1.3)b	0.06 (<0.01)b	4.56 (0.04)b	0.65 (0.02)b	0.21 (0.007)b	0.46 (0.02)a	0.3	
Pine chip	0 ^a	0.11	0.70	0.11	0.79	0.35	<0.01	0.10	1.2	
	350	0.25 (0.01)a	3.32 (0.11)a	0.14 (0.007)a	1.93 (0.06)a	0.87 (0.04)a	0.01 (<0.01)a	0.21 (0.01)a	1.9	
	500	0.35 (<0.01)b	0.05 (0.15)b	0.23 (0.10)a	2.70 (0.02)b	1.37 (0.01)b	0.04 (0.08)b	0.28 (<0.01)b	2.1	
Poultry litter	0 ^a	0.47	17.73	0.48	30.98	4.76	8.61	10.32	15.2	
	350	0.95 (0.35)a	44.3 (0.94)a	2.13 (0.16)a	58.86 (0.17)a	11.22 (0.73)a	18.78 (0.22)a	29.43 (0.21)a	15.9	
	700	0.77 (0.26)a	62.8 (1.12)b	2.56 (0.32)b	86.64 (2.02)b	12.63 (0.24)a	26.9 (0.58)b	42.79 (0.72)b	26.8	
Switchgrass	0 ^a	0.04	0.63	<0.01	4.02	0.84	0.01	0.84	4.2	
	250	0.04 (0.01)a	1.12 (0.15)a	0.05 (<0.01)a	4.87 (0.07)a	1.16 (0.05)a	0.03 (<0.01)a	1.01 (0.16)a	5.0	
	500	0.10 (<0.01)b	5.12 (0.14)b	0.15 (0.01)b	11.59 (0.05)b	3.79 (0.07)b	0.10 (0.01)b	2.39 (0.70)b	13.9	

^a Only a single measurement was collected per sample

^b Means determined from triplicate measurements were compared between lower and higher pyrolysis temperature for each feedstock using a one-way ANOVA with values followed by a different letter being significantly different at $P=0.05$

Table 4 Micro-elemental composition in raw feedstocks and biochars produced under different pyrolysis temperatures (standard deviation in parentheses)

Feedstock	Pyrolysis (°C)	Micro-elemental composition (mg kg ⁻¹) ^b										
		B	Ba	Cl ^a	Co	Cu	Mn	Mo	Se	Sn	V	Zn
Bagasse	0 ^a	0	0.2	18	0.9	14.7	5.9	0.7	0	0.2	0.2	2.2
	350	1.5 (0.3)	4.7 (0.1)a	10	0	13.9 (1.3)a	9.6 (0.3)a	0.5 (0.1)a	0	0.2 (0.2)a	0.3 (0.03)a	19 (0.8)a
	500	0.8 (<0.01)	6.6 (0.3)b	7	0.11 (0.1)	15.4 (0.8)a	14 (0.1)b	0.5 (0.2)a	0	1.8 (0.4)b	0.5 (0.1)a	26 (0.6)b
Peanut hull	0 ^a	0	12.4	7	0.3	6.0	47	4.3	0	0	0.7	2.3
	400	0	51 (1)a	14	1 (0.1)a	94 (70)a	125 (1)a	17.8 (1)a	0.8 (0.5)a	0	4.2 (0.1)a	39 (1)a
	500	0	80 (1)b	19	1.2 (0.1)a	505 (206)b	152 (0.4)b	1.5 (0.4)b	0.7 (0.4)a	0	4.9 (0.1)a	55 (2.2)a
Pecan shell	0 ^a	0	15	2	0.3	236	50	1.3	0	14.5	0.4	72
	350	0	31 (16)a	3	1 (0.1)a	7.7 (1.1)a	55 (2.1)a	0.1 (0.1)	0.7 (0.4)a	0	0	0.8 (0.8)a
	700	0	34 (0.2)a	8	2.1 (0.1)b	20.6 (3.2)b	127 (3)b	0	0.2 (0.1)a	1 (0.7)	0	0.5 (0.6)a
Pine chips	0 ^a	0	3.0	1	2	0.1	36	0	0	0.1	0	1.9
	350	6.0 (0.5)	8 (1.1)a	2	0	6 (0.5)a	83 (1.0)a	0.2 (0.1)	0	0.5 (0.2)a	0.3 (0.01)a	32 (0.6)a
	500	8.6 (0.8)	11 (0.2)b	4	0.1 (0.01)	9 (0.4)b	117 (1)b	0	0	2.6 (0.1)b	0.3 (0.02)a	44 (1.7)b
Poultry litter	0 ^a	0	33	2262	1.8	370	477	6.0	1.2	0.3	1.6	357
	350	0	122 (25)a	7898	7 (0.1)a	793 (15)a	1380 (21)a	13 (0.1)a	2.3 (0.5)a	0.2 (0.1)a	5.8 (0.1)a	812 (15)a
	700	0	137 (2.4)b	16589	10 (0.4)b	1168 (10)b	1989 (66)b	22 (0.7)b	3.3 (0.7)a	1.2 (0.6)b	8.7 (0.3)b	1200 (21)b
Switchgrass	0 ^a	0	8.7	38	0.2	5.0	29	0.2	0	0.5	0	7.0
	250	0	11 (0.1)a	29	0.1 (0.1)a	5.2 (0.5)a	37 (1)a	0.2 (0.1)a	0.6 (0.1)a	0	0	12 (0.3)a
	500	0	37 (0.2)b	121	0.6 (0.1)b	11 (0.4)b	136 (1)b	0.8 (0.1)b	0.7 (0.1)a	0	0	44 (0.4)b

^a Only a single measurement was collected per sample

^b Means determined from triplicate measurements were compared between lower and higher pyrolysis temperature for each feedstock using a one-way ANOVA with values followed by a different letter being significantly different at $P=0.05$

Table 5 Mean concentrations for trace elements in raw feedstocks and chars (standard deviations in parentheses)

Feedstock	Pyrolysis (°C)	Elemental concentration (mg kg ⁻¹) ^b					
		Ag	As	Cd	Cr	Ni	Pb
Bagasse	0 ^a	0	0	0	0.6	0.3	0.2
	350	0	0.11 (0.03)	0	1.1 (0.2)a	0.6 (0.1)a	2.2 (0.3)a
	500	0	0	0	1.3 (0.1)a	0.5 (0.1)a	3.1 (0.8)a
Peanut Hull	0 ^a	0	0.2	0	0.4	0.3	0.3
	400	0.4 (0.3)a	0.3 (0.1)a	0.2 (0.1)	11 (4)a	6.4 (2)a	1.8 (0.1)a
	500	3.6 (1.6)b	0.1 (0.1a)	0	13 (3)a	10.2 (3)a	2.6 (0.2)b
Pecan shell	0 ^a	0	0	0.6	4.3	41	37
	350	0	0	0	0.8 (0.8)a	1 (0.4)a	0.2 (0.1)a
	700	0	0	0	0.2 (0.1)a	2.8 (1)a	1 (0.7)a
Pine chip	0 ^a	0	0	0.2	0.2	0.12	0
	350	2.0 (1.8)a	0	0.2 (0.01)	0.6 (0.1)a	1.2 (0.5)a	1.7 (0.3)a
	500	1.0 (0.7)a	0	0	0.8 (0.1)a	1.1 (0.3)a	4.1 (0.4)b
Poultry litter	0 ^a	0	1.3	0.1	3	24	0.6
	350	0	2 (0.1)a	0.2 (0.1)a	20 (0.4)a	51 (1)a	2.1 (0.1)a
	700	0	2.6 (0.2)a	0.1 (0.1)a	47 (3.7)b	93 (2.3)b	2.6 (0.1)b
Switchgrass	0 ^a	0	0	0	0	0.1	1.1
	250	0	0	0	0.2 (0.2)a	1 (0.2)a	1.9 (0.4)a
	500	0	0	0	0.5 (0.2)a	9 (1.2)b	2.9 (0.1)b

^a Only a single measurement was collected per sample

^b Means determined from triplicate measurements were compared between lower and higher pyrolysis temperature for each feedstock using a one-way ANOVA with values followed by a different letter being significantly different at $P=0.05$

temperature (Table 4). Similar to the char's macro-elemental concentrations, raising the pyrolysis temperature showed mixed results on increasing micro-elements levels. For example, the Cu and Zn concentrations in the PL char both increased nearly 50% with increasing pyrolysis temperature. A few micro-nutrient concentrations, in contrast, had no impact of temperature.

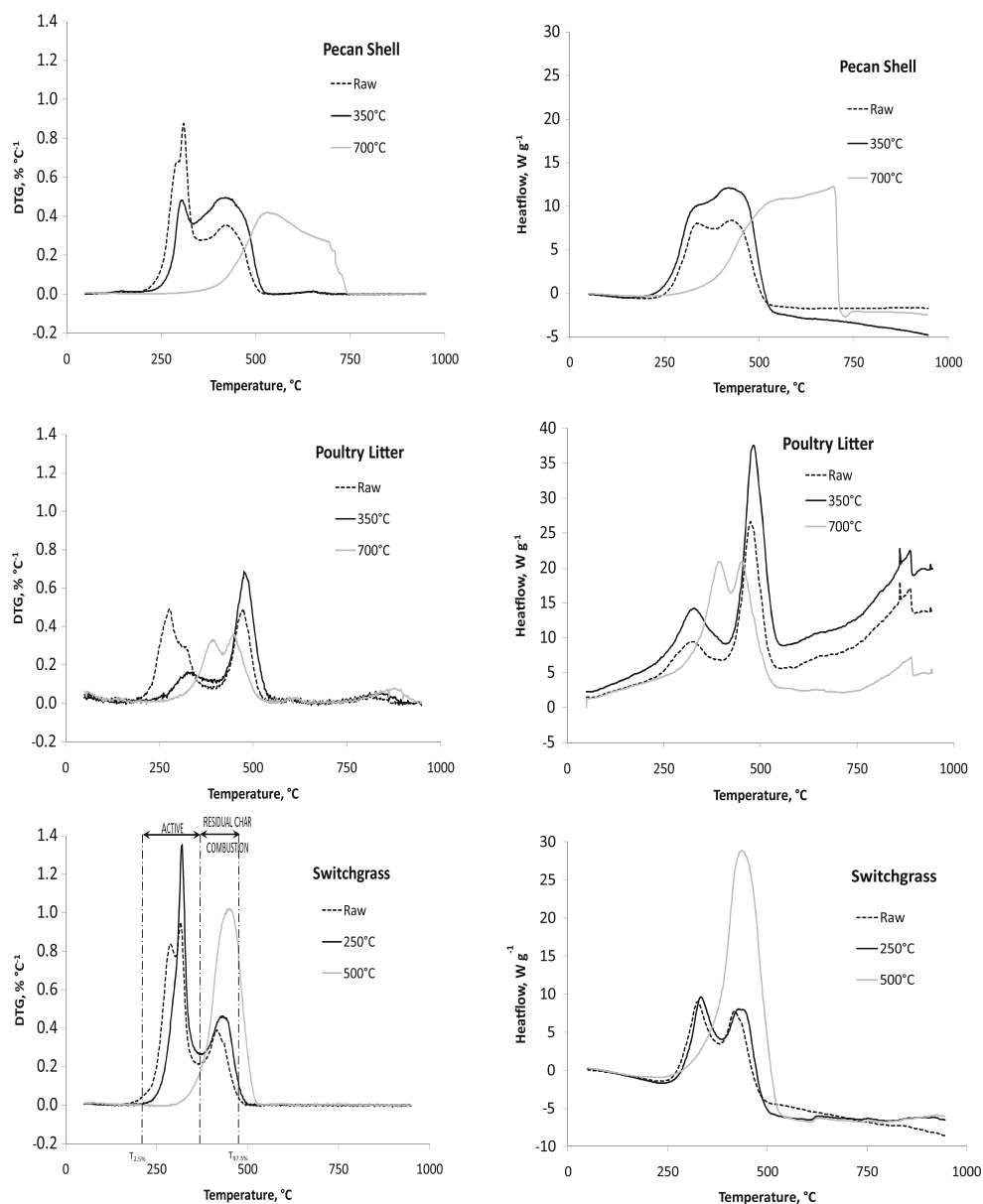
Although trace element concentrations in chars are not often scrutinized for their impact on thermal energy considerations, their presence becomes apparent when considered for use as soil amendments. Maintaining highly fertile soils through char applications requires that the chars should not contain appreciable quantities of hazardous elements. Therefore, the raw feedstocks and chars were analyzed for six of nine hazardous trace elements listed on the USEPA Code of Federal Regulations Part 503 [36]. None of the six trace element concentrations in these chars exceeded the EPA ceiling concentrations. While not exceeding the ceiling concentration, trace element accumulation in soil treated with these chars could eventually be reached after long-term, heavy applications rates. All raw feedstocks and chars contained relatively low amounts of Ag, As, Cd (<3.6 mg kg⁻¹, Table 5). In contrast, Cr and Pb occurred in modest amounts (<48 mg kg⁻¹). Nickel

was measured in both raw PL and PS at concentrations between 24 and 41 mg kg⁻¹, respectively. The Ni concentration in PS char pyrolyzed at both temperatures declined relative to the raw PS probably due to chelation by organic acids that were susceptible to vaporization as VM (Table 5). In contrast, Ni concentrations were significantly greater in PL chars with increasing pyrolysis temperature (93 mg kg⁻¹). This may be a result of salt formation with anionic species (i.e., Cl, SO₄) that were more thermally stable and resisted removal via a volatilization pathway.

Char Combustion Properties

Thermal degradation assessment of the raw feedstocks demonstrated two combustion macro-steps: an active combustion segment where there is a release of volatiles and their immediate oxidative degradation that transitioned into a char oxidation step [41, 61] (Fig. 4). Thus, two peaks occur in the DTG plots (Fig. 5) whose maxima (T_v and T_c) are identified in Table 6. In the char oxidation phase, which contains partially carbonized residue from the initial phase and the original fixed carbon, there was a slow and continuous weight loss until an average $T_{97.5\%}$ of $480 \pm 9^\circ\text{C}$ (average among plant-based feedstocks); whereas PL chars

Fig. 4 Combustion profile (DTG and DTA) of pecan shell, poultry litter, and switchgrass raw feedstock and biochar counterparts



finished with a $T_{97.5\%}$ of $521 \pm 1^\circ\text{C}$. The mass loss during the active (volatile) combustion segment can be attributed to the volatile portion undergoing a series of rapid devolatilization and oxidation reactions. Therefore, during the combustion of biomass, our results show that both pyrolysis and combustion occurred in series as evidence by the T_v being less than $T_{V_{\text{Max}}}$, the maximum heat flow temperature in the volatile combustion stage (Tables 6 and 7). The transition to the second char oxidation phase exhibited a minor plateau, especially for the raw PL and PS feedstocks (Fig. 4), signaling a constant mass loss rate (DTG value). This phase has been described as a pre-combustion or introductory region of the reaction where diffusion and beginning char combustion were taking place [62, 63].

As the individual feedstocks were pyrolyzed, the DTG curves slowly shifted from prominent dual peak curves to a

singular peak with maxima occurring at greater temperatures. This intense char combustion peak indicated both a higher char yield and catalyzed char combustion brought on by the presence of inorganic elements [64]. The previous was true for all feedstocks except PL; even at 700°C , the two combustion stages were still noticeable albeit the difference between peak temperatures decreased appreciably (Table 6). A one-way ANOVA revealed that the $T_{2.5\%}$ and T_{Ch} results were temperature regime dependent. In fact, as the char's pyrolytic temperature increased, these characteristic DTG temperatures also increased indicating an increase in required energy to begin combustion. As a consequence, the DTG curves were shifted toward the greater temperatures (Fig. 4).

For the DTA curves (Fig. 4), combustion of a feedstock was represented by two clear thermo-positive peaks. As

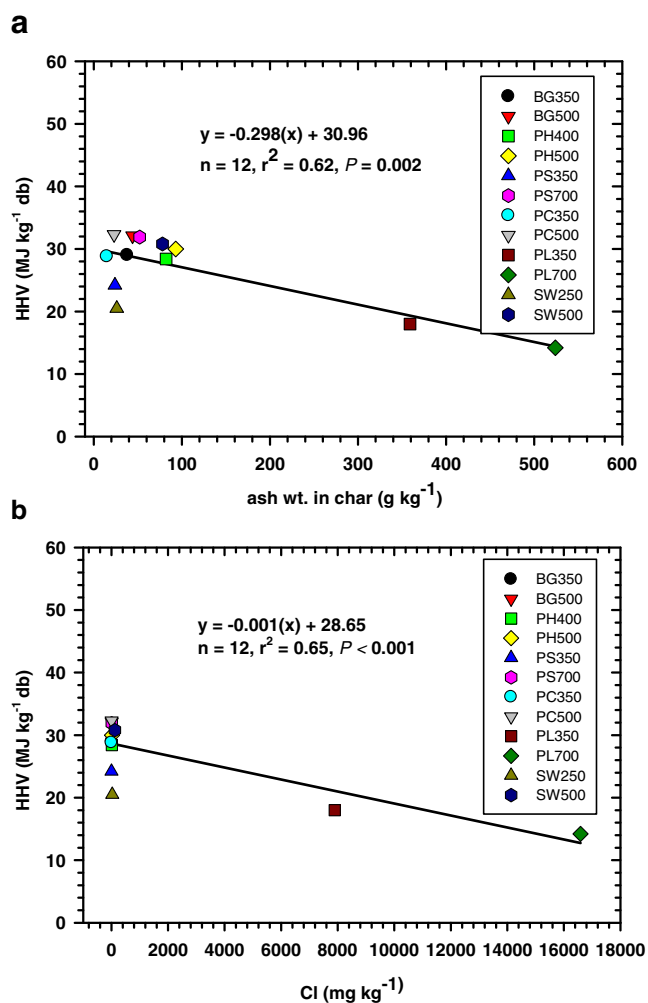


Fig. 5 Linear relationship between HHV and **a** total ash as grams per kilogram and **b** Cl as milligrams per kilogram

with the DTG curves, the DTA curves associated with the charred materials shifted toward a singular higher temperature peak indicating a more uniform material was combusting (except for PL). Concordantly, T_{Onset} and T_{Endset} increased with pyrolytic temperature (Table 7). Comparing raw feedstocks to their char counterparts, active volatile combustion produced a larger maximum differential temperature ΔT_{VMax} (except for PC). The increase in ΔT_{VMax} suggested that the volatile compounds remaining in the chars were more energy dense. The ΔT_{CMax} values of the chars were found to also increase with pyrolysis temperature, except for BG. Char from BG actually experienced a decrease in ΔT_{CMax} with an increase in pyrolysis temperature. Meanwhile, the $\Delta H_{\text{TotalRelative}}$ value for this char increased to 2.88, which was the largest change in value among the chars examined in this study.

Combustion of the chars produced greater ΔH_{Total} values relative to the raw feedstocks. As pyrolysis temperature increased for the plant- and wood-based materials, this

property increased 1.28- to 2.88-fold relative to values measured in the raw feedstock (Table 7). Poultry litter char was an improved fuel source compared to its raw counterpart ($\Delta H_{\text{TotalRelative}} = 1.44$); however, additional increases in pyrolytic temperature did not greatly improve its fuel quality ($\Delta H_{\text{TotalRelative}} = 1.40$).

Few chars (or raw feedstocks) component concentrations correlated to characteristic TG and DTA temperatures. Collectively, char T_{C} negatively correlated with both VM and H contents. The T_{Onset} was correlated with C and FC (positive) and VM and H (negative). Within a low or high temperature regime char, C and FC both had strong positive correlations with T_{V} and $T_{2.5\%}$, respectively. Conversely, H and N were found to be negatively correlated to ΔT_{CMax} .

Energy contents of the raw feedstocks and chars behaved much in the same manner as ΔH_{Total} values (Table 7). After analysis by a one-way ANOVA, the HHV and ΔH_{Total} values were found to be temperature regime dependent. Pyrolysis increased the energy content with additional temperature increases generating a more energy dense product. The PL char was also found to be statistically different than other chars largely attributed to its higher ash content and lower C content. When assessing the HHV values of the chars and raw feedstocks on a daf basis, essentially the energy content of the organic combustible material alone, materials within a temperature regime (including feedstocks) were statistically similar. As reported in this study, however, PL contains a diversity of inorganic elements that reduces its relative HHV content. Thus, washing or some other ash reducing technique could make PL as valuable an energy resource as plant-based feedstocks and associate chars [19, 65].

Kinetic parameters were assessed for the raw feedstocks and chars using Eqs. 1, 2, and 3. Because of the two macro-steps during combustion, kinetic parameters were determined for each step since one set of parameters would not accurately characterize across the entire combustion temperature range (Table 6). As shown in Table 8, no singular general trend could be reported regarding the effects of pyrolysis on the feedstocks examined. When observing the trend for the order of the reaction, n , which is the dependence of the reaction rate on one or many reactants, we found that n during char combustion (second stage) gradually reduced for BG, PL, and PS chars. This suggested that pyrolyzing these raw feedstocks generated a more uniform carbon structure. For PH and PC feedstocks, pyrolysis initially increased the reaction order and then decreased the reaction order to approach first order, where combustion would depend on only one reactant. Switchgrass demonstrated an initial decrease in reaction order when torrefied and then an increase suggesting the possible rearrangement to carbon structures when pyrolyzed at greater than 250°C that influence the combustion kinetics.

Table 6 Thermogravimetric analysis of raw feedstocks and chars (– indicates data not available)

Feedstock	Pyrolysis (°C)	Volatile combustion			Char combustion			Residual wt.% _{db}
		$T_{2.5\%}$ °C	T_V °C	DTG_V %°C ⁻¹	T_{Ch} °C	DTG_{Ch} %°C ⁻¹	$T_{97.5\%}$ °C	
Bagasse	0	254	322	1.188	440	0.376	478	0.83
	350	300	–	–	422	0.967	492	0.74
	500	366	–	–	463	1.111	512	2.00
Peanut hull	0	219	290	0.743	386	0.347	500	2.59
	400	275	–	–	428	0.578	669	5.95
	500	323	–	–	449	0.448	693	7.92
Pecan shell	0	251	308	0.790	427	0.359	636	0.85
	350	271	306	0.472	418	0.505	663	1.29
	700	419	–	–	537	0.391	772	4.01
Pine chip	0	252	318	0.978	411	0.494	488	0.00
	350	306	–	–	433	0.876	498	0.00
	500	364	–	–	463	0.849	577	0.58
Poultry litter	0	230	269	0.513	454	0.337	521	20.5
	350	277	318	0.127	445	0.309	618	32.0
	700	286	–	–	422	0.209	623	47.0
Switchgrass	0	242	308	0.923	395	0.349	474	0.73
	250	270	314	1.10	404	0.445	487	1.36
	500	363	–	–	451	1.056	506	5.41

Table 7 Differential thermal analysis and energy content of feedstocks and chars (– indicates data not available)

Feedstock	Pyrolysis (°C)	Energy content		Volatile combustion			Char combustion			ΔH_{Total} kJ g ⁻¹	$\Delta H_{TotalRelative}$
		db MJ kg ⁻¹	daf	T_{Onset} °C	ΔT_{VMax} °C	T_{VMax} °C	ΔT_{CMax} °C	T_{CMax} °C	T_{Endset} °C		
Bagasse	0	18.6	19.7	254	2.30	335	4.30	439	477	7.65	1.0
	350	29.0	30.2	283	6.95	325	11.59	424	488	20.1	2.63
	500	32.1	33.6	268	–	–	8.18	467	509	22.0	2.88
Peanut hull	0	20.5	21.3	278	15.22	318	11.05	400	492	11.68	1.0
	400	28.4	30.9	275	–	–	11.03	436	514	22.26	1.91
	500	30.0	33.1	298	–	–	12.82	455	521	24.03	2.06
Pecan shell	0	20.3	20.7	300	12.69	339	12.41	439	501	10.39	1.0
	350	24.2	24.8	258	–	–	–	435	516	16.40	1.58
	700	31.9	33.6	390	–	–	13.44	619	621	22.81	2.20
Pine chip	0	20.3	20.5	273	11.49	344	12.07	422	480	9.69	1.0
	350	28.8	29.3	241	8.46	351	12.84	438	493	19.47	2.01
	500	32.3	33.1	359	–	–	13.04	467	519	23.15	2.39
Poultry litter	0	15.0	19.8	244	3.18	312	14.96	478	530	9.03	1.0
	350	18.0	28.0	234	9.12	317	15.98	490	603	13.03	1.44
	700	14.2	29.8	303	–	–	16.19	447	571	12.67	1.40
Switchgrass	0	18.1	18.6	261	2.75	324	3.22	427	475	9.45	1.0
	250	20.5	21.1	262	4.14	335	3.70	446	482	12.09	1.28
	500	30.8	33.3	372	–	–	9.53	457	511	22.63	2.39

Table 8 Combustion kinetic parameters of raw feedstocks and chars (– indicates data not applicable)

Feedstock	Pyrolysis (°C)	Volatile combustion			Char combustion		
		$\log_e A$	E_a kJ mol ⁻¹	n	$\log_e A$	E_a kJ mol ⁻¹	n
Bagasse	0	20.0	111.5	0.94	42.8	259.6	1.65
	350	–	–	–	9.56	73.6	0.93
	500	–	–	–	16.0	115.4	0.88
Peanut hull	0	14.1	82.4	1.72	8.27	62.9	1.10
	400	–	–	–	9.12	68.6	1.82
	500	–	–	–	8.08	70.4	0.97
Pecan shell	0	18.9	105.0	0.92	21.3	134.9	1.67
	350	25.8	138.3	0.79	16.7	110.0	1.70
	700	–	–	–	4.00	58.2	1.16
Pine chip	0	16.9	97.5	0.91	22.2	142.0	1.16
	350	–	–	–	9.27	72.1	1.51
	500	–	–	–	14.0	103.8	0.99
Poultry litter	0	17.2	93.4	1.17	38.7	240.6	2.79
	350	8.83	60.8	0.60	14.1	106.8	2.04
	700	–	–	–	7.1	63.6	1.66
Switchgrass	0	27.0	140.0	3.15	22.7	142.5	1.37
	250	23.5	131.6	1.08	18.9	125.3	1.16
	500	–	–	–	20.0	136.0	1.29

With respect to E_a values for the low and high temperature char materials, PS700 char had the lowest E_a value of 58.2 kJ mol⁻¹. This was closely followed by BG350, PH400, PH500, PC350, and PL700 with average E_a values of 69.7±3.9 kJ mol⁻¹. The char requiring the greatest amount of energy to begin combustion was SG pyrolyzed at 500°C with an E_a value of 136.0 kJ mol⁻¹. Compared to their feedstock counterparts, pyrolysis decreased E_a values creating a less energy intensive combustion char feedstock.

Relationships between Char Yields, Composition, and Thermal Properties

A char's thermal properties were influenced by its total ash content as well as the quantity of individual elements in the ash [3, 15, 23]. For example, a char's high ash content along with its entrained K and Cl concentrations can lower heating values by reducing biomass conversion via the devolatilization process and by acting as a heat sink that lowers thermal efficiencies [60]. Therefore, our results were examined for similar impacts of ash contents on char yields and HHV results. A Pearson Product Moment Correlation analysis revealed no significant relationship between the collective ($n=12$) char yields expressed on a mass or C basis (%_{db}) and the char's total ash content nor the concentration of individual elements measured in the ash (all r^2 and P values were <0.09 and >0.05, respectively). The lack of a relationship between these variables was unexpected

considering others reported significant associations between char yields and ash characteristics [3, 15, 23].

Using each char's HHV properties, a Pearson Product Moment Correlation test revealed that there was a relationship with the char's total ash contents, and only with the char's Cl concentration. There was no significant relationship between each char's HHV and the remaining individual elements (i.e., Al, Ca, Fe, K, Mg, Na, P, S, Si, and Zn) entrained within the ash. The chars' HHV relationship with their total ash content and Cl concentration were further refined using linear regression analyses (Fig. 5a, b). A significant inverse linear relationship occurred between the chars' HHV properties and their total ash and Cl contents. This is a well-known concept in the biomass thermal energy literature and corroborates that each char's thermal characteristics decline with higher ash and Cl contents entrained with the ash. Additional analyses using polynomial regression models did not improve (higher r^2 or lower P value) the predictive fit between the chars HHV and their ash characteristics.

Conclusions

Char yields, thermal energy values, and both the inorganic and organic characteristics were influenced by raw lignocellulosic and PL feedstock selection and by choice of pyrolysis temperature. Slow pyrolysis of six common raw feedstocks from the Southeastern USA using a low

(≤ 400 °C) and high (≥ 500 °C) temperature regime resulted in char yields on a mass and C basis of between 28%_{db} and almost 80%_{db}. The higher pyrolysis temperature resulted in lower char yields, caused the chars to have elevated ash contents, alkaline pH values, more aromatic character, and narrow O/C and H/C ratios.

All raw feedstocks and chars contained mixed amounts of macro-, micro-, and trace element concentrations, and it was difficult to express compositional generalities about four of the raw feedstocks. But, for two of the feedstocks, there were large differences in compositional characteristics. Char made from PC had among the lowest macro-, micro-, and trace element compositions, but had some exceptional HHV values. In this study, the raw PL feedstock and its chars showed the highest diversity and largest concentration of inorganic elements within all the examined feedstocks and chars.

Pyrolysis of these common lignocellulosic and litter feedstocks generated a char product whose characteristic combustion temperatures were found to correlate to its C, H, and N contents. As the char's pyrolysis temperature increased, DTG and DTA combustion curves shifted upward towards higher temperature peaks indicating combustion of a more uniform material. Chars HHV tended to increase with heightened pyrolysis temperature with some chars producing >30 MJ kg⁻¹. The chars' HHV characteristics were significantly inversely correlated with the chars total ash and Cl contents.

Combustion kinetics parameters were found to vary with feedstock and pyrolysis temperature with SG chars having the greatest E_a values for combustion. Based upon the order of reaction, n , pyrolysis of lignocellulosic and poultry litter feedstocks gradually declined with increasing temperature, suggesting the creation of a more uniform product. This allows for the characterization of combustion kinetics among our samples to be based upon a single reactant.

Lignocelluloses chars had more suitable thermal characteristics and lower mineral matter, implying acceptable service in thermal energy production. In contrast, PL char obtained from one source had relatively medium HHV values for energy applications and its assortment of inorganic elements will cause additional technical difficulties. These difficulties arise from this PL char having greater ash contents and containing corrosive inorganic elements that renders it problematic with maintaining the thermal integrity of downstream energy conversion and clean-up equipment. Nevertheless, these characteristics could be overcome through additional processing such as quick wash with water or alkali agents or addition of amendments to capture the alkali elements [3]. Here, our results show that it would be prudent to determine the total elemental composition and structural characteristics of raw feedstocks before pyrolysis, thus allowing for an assessment of their suitability for

thermal energy processing without jeopardizing the mechanical integrity of downstream processing equipment. In turn, feedstock selection and pyrolysis temperatures can be selected to insure that char ash amounts and qualitative characteristics do not detract from obtaining optimum thermal energy production and fuel yield recoveries.

Acknowledgments This publication is based on work supported by the US Department of Agriculture, Agriculture Research Service, and under the ARS-GRACEnet project. The authors express gratitude to collaborators who manufactured the chars used in this study and to Barry Glaz, Jerry H. Martin II and Sheeneka Green in sample preparation and analyses.

References

- Demirbas A, Arin G (2002) An overview of biomass pyrolysis. *Energy Sources* 24:471–482
- Boateng AA (2007) Characterization and thermal conversion of charcoal derived from fluidized-bed fast pyrolysis oil production of switchgrass. *Ind Eng Chem Res* 46:8857–8862
- Khan AA, de Jong W, Jansens PJ, Spliethoff H (2009) Biomass combustion in fluidized bed boilers: potential problems and remedies. *Fuel Process Technol* 90:21–50
- Lv D, Xu M, Liu X, Zhan Z, Li Z, Yao H (2010) Effect of cellulose, lignin, alkali and alkaline earth metallic species on biomass pyrolysis and gasification. *Fuel Proc Technol* 91:903–909
- Ro KS, Cantrell KB, Hunt PG (2010) High-temperature pyrolysis of blended animal manure for producing renewable energy and value added biochar. *Ind Eng Chem Res* 49:10125–10131
- Antal MJ, Grønli M (2003) The art, science, and technology of charcoal production. *Ind Eng Chem Res* 42:1619–1640
- Brown R (2009) Biochar production technology. Biochar for environmental management. In: Lehmann J, Joseph S (eds) *Biochar for environmental management science and technology*. Earthscan, London
- Sohi S, Lopez-Capel E, Krull E, Bol R (2009) Biochar, climate change and soil: a review to guide future research. CSIRO, Glen Osmond, Australia. Available at: <http://www.csiro.au/files/files/poei.pdf>. Accessed 24 April 2012
- Boateng AA, Mullen CA, Goldberg N, Hicks KB, Jung HJ, Lamb JF (2008) Production of biofuel from alfalfa stems by fluidized-bed fast pyrolysis. *Ind Eng Chem Res* 47:4115–4122
- Lehmann J (2007) Bio-energy in the black. *Front Ecol Environ* 5:381–387
- Laird DA (2008) The charcoal vision: a win-win-win scenario for simultaneously producing bioenergy, permanently sequestering carbon, while improving soil and water quality. *Agron J* 100:178–181
- Novak JM, Busscher WJ, Laird DL, Ahmedna M, Watts DW, Niandou MAS (2009) Impact of biochar amendment on fertility of a southeastern coastal plain soil. *Soil Sci* 174:105–112
- Whitehead DC (2000) Nutrient elements in grasslands: soil-plant-animal relationships. CABI, New York
- Sistani KR, Novak JM (2006) Trace metal accumulation, movement and remediation in soils receiving animal manure. In: Prasad MN, Sajwan KS, Naidu R (eds) *Trace elements in the environment, biogeochemistry, biotechnology, and bioremediation*. CRC, Boca Raton
- Novak JM, Lima IM, Xing B, Gaskin JW, Steiner C, Das KC et al (2009) Characterization of designer biochar produced at different

- temperatures and their effects on a loamy sand. *Ann Environ Sci* 3:195–206
16. Obernberger F, Biedermann F, Widmann W, Riedl R (1997) Concentrations of inorganic elements in biomass fuels and recovery in the different ash fractions. *Biomass Bioenergy* 12:211–224
 17. Demirbas A (2004) Effects of temperature and particle size on biochar yield from pyrolysis of agricultural residues. *J Anal Appl Pyrol* 72:243–248
 18. Gaskin JW, Steiner C, Harris K, Das KC, Bibens B (2008) Effect of low-temperature pyrolysis conditions on biochar for agriculture use. *Trans ASABE* 51:2061–2069
 19. Arvelakis S, Koukios EG (2002) Physiochemical upgrading of agro-residues as feedstocks for energy production via thermochemical conversion methods. *Biomass Bioenergy* 22:331–348
 20. Fahmi R, Bridgewater I, Donnison I, Yates N, Jones JM (2008) The effect of lignin and inorganic species in biomass on pyrolysis oil yields, quality, and stability. *Fuel* 87:1230–1240
 21. Raveendran K, Ganesh A, Khilar KC (1996) Pyrolysis characteristics of biomass and biomass components. *Fuel* 75:987–998
 22. Quyn DM, Wu HW, Bhattacharya SP, Li CZ (2002) Volatilization and catalytic effects of alkali and alkaline earth metallic species during pyrolysis and gasification of Victorian brown coal. Part II. Effect of chemical form and valence. *Fuel* 81:151–158
 23. Wu HW, Quyn DM, Li CZ (2002) Volatilization and catalytic effects of alkali and alkaline earth metallic species during the pyrolysis and gasification of Victorian brown coal. Part III. The importance of the interaction between volatiles and char at high temperature. *Fuel* 81:1033–1039
 24. Milesi C, Elvidge CD, Nemani RR, Running SW (2003) Assessing the impact of urban land development on net primary productivity in the southeastern United States. *Remote Sens Environ* 86:401–410
 25. USDA (2010) A USDA Regional Roadmap to Meeting the Biofuel Goals of the Renewable Fuels Standard by 2022. Available at: http://www.usda.gov/documents/USDA_Biofuel_Report_6232010.pdf. Accessed 24 April 2012
 26. Kellogg RL, Lander CH, Moffitt DC, Gollehon N (2000) Manure nutrients relative to the capacity of cropland and pastureland to assimilate nutrients: Spatial and temporal trends for the United States. USDA-NRCS-ERS-Publ. No. NPS00-0579
 27. Cantrell KB, Martin JH (2012) State-space temperature regulation development of biochar production Part II: Application to manure processing via pyrolysis. *J Sci Food Agric* 92:490–495
 28. Lima IM, Marshall WE (2005) Granular activated carbon from broiler manure: physical, chemical, and absorptive properties. *Bioresour Technol* 96:699–706
 29. Toles CA, Marshall WE, Johns MM (1998) Phosphoric acid activation of nutshells for metals and organic remediation: process optimization. *J Chem Technol Biotechnol* 72:255–263
 30. Bergman PCA, Kiel JHA (2005) Torrefaction for biomass upgrading. 14th European Biomass Conference, Paris, France. 17–21 October 2005. Available at: <http://www.ecn.nl/docs/library/report/2005/rx-0180.pdf>. Accessed 24 April 2012
 31. Bourgeois J, Guyonnet R (1988) Characterization and analysis of torrefied wood. *Wood Sci Technol* 22:143–155
 32. Bridgeman TC, Jones JM, Williams A, Waldron DJ (2010) An investigation of the grindability of two torrefied energy crops. *Fuel* 89:3911–3918
 33. Phanphanich M, Mani S (2011) Impact of torrefaction on the grindability and fuel characteristics of forest biomass. *Bioresour Technol* 102:1246–1253
 34. Repellin V, Govin A, Rolland M, Guyonnet R (2010) Energy requirement for fine grinding of torrefied wood. *Biomass Bioenergy* 34:923–930
 35. ASTM (2006) Petroleum products, lubricants, and fossil fuels: gaseous fuels, coal, and coke. ASTM, West Conshohocken, PA
 36. USEPA (2005) Title 40—Protection of Environment. Standards for the use or disposal of sewage sludge. Code of Federal Regulations. Title 40, Pt. 503. US Environmental Protection Agency, Washington, DC
 37. USEPA (1996) Test methods for evaluating solid waste, physical/chemical methods. Methods SW-846 Method 3052: microwave assisted acid digestions of siliceous and organically based matrices. Available at: <http://www.epa.gov/osw/hazard/testmethods/sw846/pdfs/3052.pdf>. Accessed 24 April 2012
 38. Wang X, Cook S, Tao S, Xing B (2007) Sorption of organic contaminants by biopolymers: role of polarity, structure and domain spatial arrangement. *Chemosphere* 66:1476–1484
 39. Cantrell KB, Martin JH, Ro KS (2010) Application of thermogravimetric analysis for the proximate analysis of livestock wastes. *J ASTM Int* 7: Paper ID JAI102583
 40. Biagini E, Barontini F, Tognotti L (2006) Devolatilization of biomass fuels and biomass components studies by TG/FTIR technique. *Ind Eng Chem Res* 45:4486–4493
 41. Cantrell KB, Hunt PG, Ro KS, Stone KC, Vanotti MB, Burns JC (2010) Thermogravimetric characterization of irrigated Bermuda grass as a combustion feedstock. *Trans ASABE* 53:413–420
 42. Bridgeman TG, Jones JM, Shield I, Williams PT (2008) Torrefaction of reed canary grass, wheat straw and willow to enhance solid fuel qualities and combustion properties. *Fuel* 87:844–856
 43. Ergundenler A, Ghaly AE (1992) Determination of reaction kinetics of wheat straw using thermogravimetric analysis. *Appl Biochem Biotechnol* 34(35):75–91
 44. Liu Q, Wang S, Zheng Y, Luo Z, Cen K (2008) Mechanism study of wood lignin pyrolysis by using TG–FTIR analyses. *J Anal Appl Pyrol* 82:170–177
 45. González JF, Román S, Encinar JM, Martínez G (2009) Pyrolysis of various biomass residues and char utilization for the production of activated carbons. *J Anal Appl Pyrol* 85:131–141
 46. Libra JA, Ro KS, Kammann C, Funke A, Berge ND, Neubauer Y et al (2011) Hydrothermal carbonization of biomass residuals: a comparative review of the chemistry, processes and application of wet and dry pyrolysis. *Biofuels* 2:89–124
 47. Cao X, Ro KS, Chappell M, Li Y, Mao J (2011) Chemical structures of swine-manure char produced under different carbonization conditions investigated by advanced solid-state ¹³C nuclear magnetic resonance (NMR) spectroscopy. *Energy Fuel* 25:388–397
 48. Inyang M, Gao B, Pullammanappallil P, Ding W, Zimmerman AR (2010) Biochar from anaerobically digested sugar cane bagasse. *Bioresour Technol* 101:8868–8872
 49. Yan Q, Toghiani H, Yu F, Cai Z, Zhang J (2011) Effects of pyrolysis conditions on yield of bio-chars from pine chips. *For Prod J* 5:367–371
 50. Parikh J, Channiwalla S, Ghosal G (2005) A correlation for calculating HHV from proximate analysis of solid fuels. *Fuel* 84:487–494
 51. Nahm KH (2003) Evaluation of nitrogen content in poultry manure. *World Poult Sci J* 59:77–88
 52. Asadullah M, Zhang S, Min Z, Yimsiri P, Li C-Z (2010) Effect of biomass char structures on its gasification reactivity. *Bioresour Technol* 101:7935–7943
 53. Spokas KA, Cantrell KB, Novak JM, Archer DW, Ippolito JA, Collins HP et al (2011) Biochar: a synthesis of its agronomic impact beyond carbon sequestration. *J Environ Qual* 41:973–989
 54. Glaser B, Lehmann J, Zech W (2002) Ameliorating physical and chemical properties of highly weathered soil in the tropics with charcoal—a review. *Biol Fertil Soils* 35:219–230
 55. Baldock JA, Smernik RJ (2002) Chemical composition and bio-availability of thermally altered *Pinus resinosa* (red pine) wood. *Org Geochem* 33:1093–1109

56. Sun H, Hockaday WC, Masiello CA, Zygourakis K (2012) Multiple controls on the chemical and physical structures of biochars. *Ind Eng Chem Res* 51:3587–3597
57. Keiluweit M, Nico PS, Johnson MG, Kleber M (2010) Dynamic molecular structure of plant biomass-derived black carbon (biochar). *Environ Sci Technol* 44:1247–1253
58. Zolin A, Jensen A, Jensen PA, Frandsen F, Dim-Johansen K (2001) The influence of inorganic materials on the thermal deactivation of fuel chars. *Energy Fuel* 15:1110–1122
59. Jenkins BM, Baxter LL, Miles TR Jr, Miles TR (1998) Combustion properties of biomass. *Fuel Process Technol* 54:17–46
60. Demirbas A (2005) Potential applications of renewable energy sources, biomass combustion problems in boiler power systems and combustion related environmental issues. *Prog Energy Combust Sci* 31:171–192
61. Wang C, Wang Q, Yang Q, Liang R (2009) Thermogravimetric studies of the behavior of wheat straw with added coal during combustion. *Biomass Bioenergy* 33:50–56
62. Chen Y, Mori S, Pan WP (1995) Estimating the combustibility of various coals by TG–DTA. *Energy Fuel* 9:71–74
63. Whitely N, Ozao R, Artiaga R, Cao Y, Pan WP (2006) Multi-utilization of chicken litter as a biomass source. Part I. Combustion. *Energy Fuel* 20:2660–2665
64. Fahmi R, Bridgewater A, Darvell L, Jones J, Yates N, Thain S et al (2007) The effect of alkali metals on combustion and pyrolysis of *Lolium* and *Festuca* grasses, switchgrass, and willow. *Fuel* 86:1560–1569
65. Hwang IH, Nakajima D, Matsuto T, Sugimoto T (2008) Improving the quality of waste-derived char by removing ash. *Waste Manage* 28:424–434